

## GMR OF STRANDED MULTIZONE CONDUCTORS

Y. Yang, S. Fortin, J. Ma, and F. P. Dawalibi  
Safe Engineering Services & technologies ltd.  
1544 Viel, Montreal, Quebec, Canada, H3M 1G4  
Tel.: (514) 336-2511 Fax: (514) 336-6144 E-mail: info@sestech.com

### ABSTRACT

This paper presents a complete solution for the computation of the GMR of stranded conductors of circular cross-section, taking the frequency dependence (skin effect) into account. The stranded conductors can consist of several zones; the radius, resistivity and permeability of the strands can be different for each zone. Results for the GMR of various conductor configurations computed with this method are presented as a function of frequency. The computation results are in good agreement with published data.

### KEY WORDS

GMR, multizone, stranded conductor, strand pattern, current density, frequency dependence.

## 1. Introduction

The Geometric Mean Radius (GMR) of a conductor is the radius of the equivalent hollow conductor with zero thickness, thus producing no internal flux, having the same self inductance as the conductor. This concept is especially useful in the computation of the internal reactance of composite or stranded conductors.

Several publications discuss the computation of the GMR of stranded conductors (and its frequency dependence) for the case where all the strands in the conductors are identical [1~3]. In this paper, a complete solution for the accurate computation of the GMR of a stranded conductor with circular cross-section is developed. The conductor can consist of several concentric tubular zones, each containing one or more concentric layers of identical strands. The radius, resistivity and permeability of the strands can be different for each zone.

The effect of the non-uniform current distribution inside the conductor, due to both the material and the frequency, is accounted for.

## 2. GMR of a Multizone Stranded Conductor

Figure 1 shows a cross-section of a “multizone” stranded conductor. The specific conductor shown in the figure has

three zones. Zone 1 and 2 both have two layers of strands, while Zone 3 has a single layer. The innermost zone is usually referred to as the *core*. Generally, the core need not contain any strands, i.e. it may be empty or be occupied by a dielectric medium.

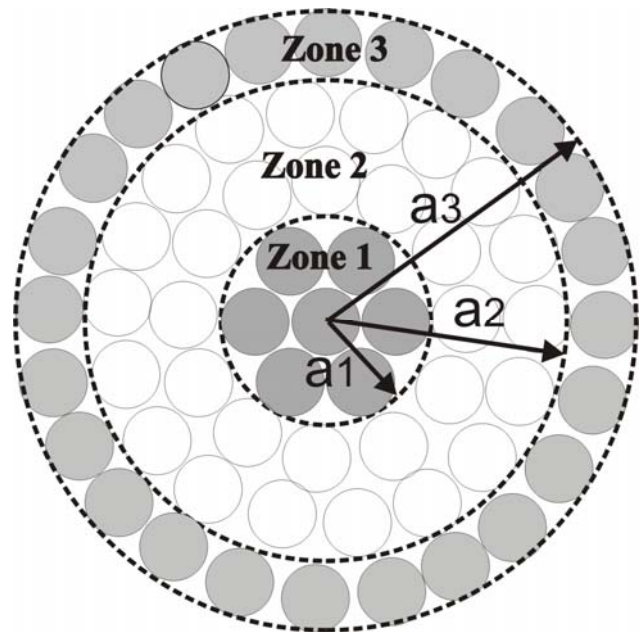


Figure 1: Stranded conductor with 3 tubular zones

Zone  $i$  is characterized by the following parameters:

- Outer radius  $a_i$  of the zone.
- Number of layers in the zone.
- Radius  $r_i$  of the strands in the zone.
- Resistivity  $\rho_i$  of the strands in the zone.
- Relative permeability  $\mu_i$  of the strands in the zone.

### 2.1 Strand Patterns

In order to obtain compact conductors, the strands are normally organized according to certain patterns. These are distinguished by the number of strands located in the first layer: either 1, 3 or 4. For each pattern, the total number of strands in the core can only be one of a specific set of numbers:

Pattern 1: 1, 7, 19, 37, 61, ...  
 Pattern 2: 3, 12, 27, 48, ...  
 Pattern 3: 4, 14, 30, 52, ...

Table 1 shows the total number of strands in the core and the number of strands in the outer layer of the core for each pattern. In the table,  $N$  is the number of layers in the core.

Table 1. Strand arrangements in different patterns

Pattern No.	View	Total number of strands in the core	Number of strands in core outer layer
1		$3N(N-1) + 1$	$1 \quad (N=1)$ $6(N-1) \quad (N>1)$
2		$3N^2$	$6(N-1) + 3$
3		$(3N+1)N$	$1 \quad (N=1)$ $6(N-1)+1 \quad (N>1)$

For layers that are outside the core, the number of strands  $N_i$  in the layer is related to the strand radius by:

$$N_i = \text{int} \left[ \frac{(R_m + r_1)\pi}{r_1} \right]$$

where  $r_1$  is the strand radius and  $R_m$  is the inner radius of the layer.

## 2.2 GMR of a Single Strand and a Single Layer

The formula for computing the GMR  $r'$  of a single strand is [4]:

$$r' = r_1 \cdot e^{-\mu_r/4} \quad (1)$$

where  $r_1$  is the radius of the strand and  $\mu_r$  is the relative permeability of the strand. This formula is valid when the current density is uniform over the cross-section of the conductor. This condition is satisfied for DC currents. It is also approximately satisfied for alternating currents, as long as the strand radius is sufficiently small. For example, a 1 cm aluminum strand has a GMR of 7.776 mm for DC, and 7.857 mm at 60 Hz. The difference is about 1%. In practice, the radius of the strands in a stranded conductor is usually much smaller than 1 cm; as a result, the error incurred by using equation (1) to calculate the GMR of individual strands is considerably smaller than 1%. In this paper, this equation is used to compute the GMR of individual strands for all frequencies. However, a more accurate expression can be used for very high frequencies, if necessary.

The GMR  $r_b$  of a single layer of  $n$  strands equally spaced along the circumference of a circle is given by [4]:

$$\begin{aligned} r_b &= \sqrt[n]{nr_q^{n-1}r'} \\ &= r_q \cdot \sqrt[n]{n \frac{r'}{r_q}} \end{aligned} \quad (2)$$

where  $r_q$  is the radius of the circle.

## 2.3 Total GMR of Conductor

The total GMR of the conductor is obtained by combining the GMR of all the layers, accounting for the fraction of current flowing in each layer. This can be done recursively, starting from the innermost layer. The GMR of the innermost layer is given by equation (2), or equation (1) if the layer consists of a single strand. The combined GMR of all the strands up to and including layer  $i$  is given by [2]:

$$GMR_i = (GMR_{i-1})^{\alpha_i} r_{bi}^{\beta_i} (d_{(i-1)i})^{2\alpha_i - \beta_i} \quad (3)$$

where  $GMR_i$  is the resultant GMR,  $GMR_{i-1}$  is the total GMR inside layer  $i$  (excluding layer  $i$ ) and  $d_{(i-1)i} = N_i r_i / \pi$  is the GMD between the strands inside layer  $i$  (excluding layer  $i$ ) and those in layer  $i$ .

The factors  $\alpha$  and  $\beta$  appearing in the exponents in equation (3) account for the fraction of current flowing in layer  $i$ :

$$\begin{aligned} \alpha_i &= \frac{I_{i-1}}{I_i} \\ \beta_i &= 1 - \alpha_i \end{aligned}$$

where  $I_i$  is the sum of the current in layers 1 to  $i$ , i.e.

$$I_i = \sum_{j=1}^i N_j \pi r_j^2 J_z(R_j) \quad (4)$$

with  $R_j$  being the distance of the center of layer  $j$  to the center of the conductor, and  $k_j$  being the number of the zone containing layer  $j$ .

## 3. Current Density Distribution Inside the Conductor

Equation (3) requires the knowledge of the current flowing in each strand. This current is given by the product of the current density and the cross-sectional area of the strand. When the frequency is zero and the properties of the material are uniform, the current density is also uniform inside the conductor and the factors  $\alpha$  and  $\beta$  in equation (3) become simple ratios of cross-sectional areas. However, when this assumption is not satisfied, the current density is not uniform, and must be calculated in a more detailed way. This section describes the technique used to estimate the current flowing in each strand for this case.

When the strands inside the conductor are in good contact, each zone can be approximated by a uniform tubular layer with the same material characteristics as the strands in the zone. The idea is then to compute the current distribution in this multilayer tubular conductor, and use the resulting current density as an estimate of the current flowing in each strand.

Note that this approach tends to underestimate somewhat the absolute value of the current density in the strands for a given injection current; however, the ratio of the current densities in different strands (which is all that is needed in equation (3)), is quite insensitive to this approximation.

Since the current distribution inside a concentric multilayer conductor is of interest in its own right, the derivation will be presented in some detail.

### 3.1 Current Density Equations and Boundary Conditions

For a very long conductor, the only non-zero component of the current density vector inside the conductor is parallel to the axis of the conductor, here taken to be the  $Z$  axis of a cylindrical coordinate system. By symmetry, the current density inside the conductor is a function of the radial distance  $r$  only. In each zone, the current must satisfy Helmholtz equation:

$$\nabla^2 J_{zi} - k_i^2 J_{zi} = 0$$

where  $k_i = \sqrt{j\omega\mu_i(1/\rho_i + j\omega\varepsilon_i)}$ ,  $\omega$  is the angular frequency and, as before,  $\mu_i$  is the permeability,  $\rho_i$  the resistivity and  $\varepsilon_i$  the permittivity of the material in zone  $i$ .

The solution of this equation takes the following general form:

$$J_{zi} = A_i I_0(k_i r) + B_i K_0(k_i r) \quad (5)$$

where  $A_i$  and  $B_i$  are unknown coefficients, with  $B_1 \equiv 0$  in order for the solution to remain finite at  $r = 0$ . In this expression,  $I_0$  and  $K_0$  are the zeroth order modified Bessel functions.

The field components resulting from this current are:

$$\begin{aligned} E_z &= \rho J_z \\ H_\phi &= j \frac{\rho}{\mu\omega} \frac{\partial J_z}{\partial r} \hat{e}_\phi \end{aligned} \quad (6)$$

The continuity of the tangential components of the electric and magnetic fields at the interfaces between the zones implies the following boundary conditions:

$$\begin{aligned} E_{zi} |_{r=a_i} &= E_{zi+1} |_{r=a_i} \longrightarrow \rho_i J_{zi} |_{r=a_i} = \rho_{i+1} J_{zi+1} |_{r=a_i} \\ H_{\phi i} |_{r=a_i} &= H_{\phi i+1} |_{r=a_i} \longrightarrow j \frac{\rho_i}{\mu_i \omega} J'_{zi} |_{r=a_i} = j \frac{\rho_{i+1}}{\mu_{i+1} \omega} J'_{zi+1} |_{r=a_i} \end{aligned} \quad (7)$$

Along with Ampere's law applied at the outer radius of the conductor, i.e.

$$H_{\phi n} |_{r=a_n} = I / 2\pi a_n$$

where  $I$  is the total current injected in the conductor, this leads to the following system of equations:

$$\begin{bmatrix} Ej_{11} & -Ej_{12} & -Ey_{12} & 0 & 0 & \cdots & 0 & 0 & \begin{bmatrix} A_1 \\ A_2 \\ B_2 \\ \vdots \\ A_n \\ B_n \end{bmatrix} \\ Mj_{11} & -Mj_{12} & -My_{12} & 0 & 0 & \cdots & 0 & 0 & \\ 0 & Ej_{22} & Ey_{22} & -Ej_{23} & -Ey_{23} & \cdots & 0 & 0 & \\ 0 & Mj_{22} & My_{22} & -Mj_{23} & -My_{23} & \cdots & 0 & 0 & \\ \vdots & \vdots & \vdots & \vdots & \vdots & \ddots & \vdots & \vdots & \\ 0 & 0 & 0 & 0 & 0 & \cdots & Mj_{nn} & My_{nn} & \end{bmatrix} = \begin{bmatrix} 0 \\ 0 \\ 0 \\ \vdots \\ 0 \\ I / 2\pi a_n \end{bmatrix}$$

where

$$\begin{aligned} Ej_{ij} &= \rho_j I_0(k_j a_i) \\ Ey_{ij} &= \rho_j K_0(k_j a_i) \\ Mj_{ij} &= j \frac{\rho_j}{\mu_j \omega} I_1(k_j a_i) \\ My_{ij} &= -j \frac{\rho_j}{\mu_j \omega} K_1(k_j a_i) \end{aligned}$$

Solving this system of equations for the coefficients  $[A_1, A_2, B_2, \dots, A_n, B_n]$  and inserting them into (4) yields the desired current density distribution.

### 3.2 Example: Current Density Distribution of a Conductor with Four Zones

As an example of the use of the method described in the previous section, Figure 2 shows the computed current density distribution for a 4-zone conductor. The radii of the zones are  $a_1 = 0.01$  m,  $a_2 = 0.02$  m,  $a_3 = 0.03$  m and  $a_4 = 0.04$  m; the relative resistivities (with respect to the resistivity of copper:  $1.724 \times 10^{-8}$   $\Omega$ -m) are:  $\rho_1 = 1$ ,  $\rho_2 = 2$ ,  $\rho_3 = 3$  and  $\rho_4 = 4$ ; the relative permeabilities with respect to air are:  $\mu_{r1} = \mu_{r2} = \mu_{r3} = \mu_{r4} = 1$ . The total injected current is 100 A. The current density distribution is computed at four frequencies: 0.01 Hz, 60 Hz, 100 Hz and 200 Hz.

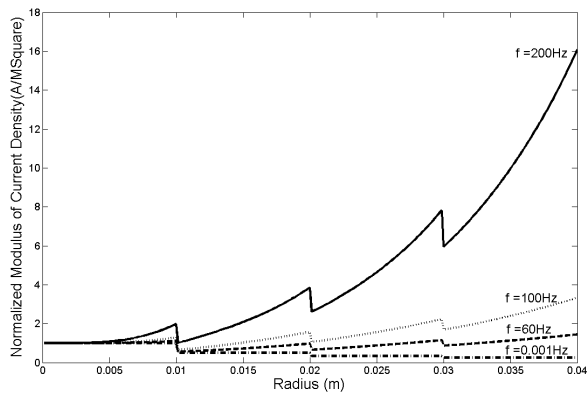


Figure 2: Normalized modulus of current density as a function of radial distance from center

In the figure, the curves are normalized by the current density at the center point  $r = 0$ . Due to the skin effect, the current density is larger towards the outer edge of each zone, and towards the outer radius of the conductor as a whole. As will be seen in the next section, this effect leads to an increase of the GMR of the conductor.

## 4. Computation Results and Comparisons

### 4.1 Computation Results

To illustrate the GMR calculation method, the GMR of a 4-zone stranded conductor is computed as a function of frequency. Three cases are considered, as shown in Table 2. In Case 1, the resistivity decreases from the inner zones to the outer zones. In Case 2, the strands are identical in all zones. In Case 3, the resistivity increases from the inner zones to the outer zones. The number of strands in each zone and the radius of the strands is the same for all cases.

Table 2. Strand Information for a 4-Zone Stranded Conductor

Zone No.	Number of Strands	Strand Radius (mm)	Relative Resistivity			$\mu_r$
			Case 1	Case 2	Case 3	
1	19	1	4	1	1	1
2	36	1	3	1	2	1
3	62	1	2	1	3	1
4	86	1	1	1	4	1

There are 3 layers in zone 1 and 2 layers in each of the other zones. The over all radius of the conductor is 0.017 m. Figure 3 shows the ratio of the GMR to the overall radius for the three cases. It can be seen that Case 1 has the largest GMR at zero frequency. This is because there is less current in the central zone, as a result of its higher resistivity. In Case 2, the strands in all four zones are the same. The computed result for the ratio is 0.7760.

This is very close to the ratio of a uniform solid conductor, which is 0.7788. When the frequency increases, the ratio also increases and gets closer to 1. The results for Case 1 and Case 2 are almost the same at high frequencies. This is because the resistivity of the outermost zone is the same for those two cases, and the current is essentially confined to the outermost zone at high frequencies.

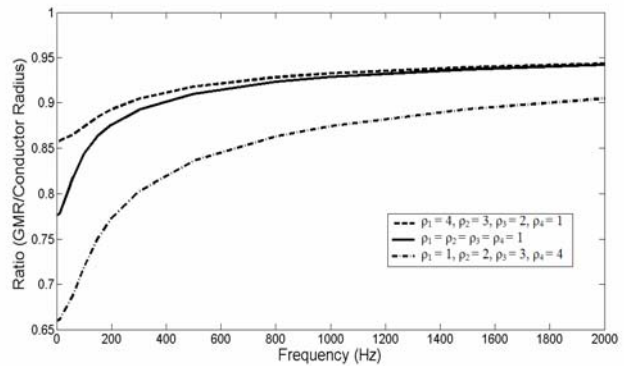


Figure 3: Ratio of GMR to the overall radius of the conductor as a function of frequency

### 4.2 Comparison with Published Data

This section uses the method presented in this paper to compute the GMR of four stranded conductors for which the value of the GMR is available in the literature. The data for the conductors are listed in Table 3. In the computations, the relative permeability and resistivity of the copper strands were set to 1, the relative permeability and resistivity of the steel strands were set to 250 and 12.5, respectively, and the relative permeability and resistivity of the aluminum strands were set to 1 and 1.6, respectively.

Table 3. Comparison between New Approach and Published Data

	Number of Strands	Radii of Strands (mm)	Published GMR (cm)	Computed GMR (cm)		
				0.001 Hz	60 Hz	1000 Hz
4/0 (Stranded Copper)	19	1.34	0.508	0.508	0.509	0.554
Baldplate	7/30	2.19/2.19	1.27	1.25	1.26	1.35
Bittern	7/45	1.42 /2.13	1.36	1.35	1.38	1.53
Bluebird	19/84	1.22 /2.03	1.79	1.78	1.86	2.05

The results agree with the published data at low frequencies. The table also lists the computed GMR value for those conductors at 1000 Hz. As expected, the high-frequency value is larger in all cases.

## 5. Conclusion

This paper introduces a method for the computation of the GMR of stranded conductors of circular cross-section consisting of several zones with distinct electrical properties. The method also accounts for frequency effects. Examples of the use of this method were presented, and shown to agree with published data.

This method can be used to provide more accurate estimates of the GMR for composite conductors made of strands of different size and properties, and also to better calculate the impedance of those conductors at higher frequencies.

## Acknowledgements

The authors would like to thank Safe Engineering Services & technologies ltd. for the financial support and resources provided during this research work.

## References

- [1] W. A. Lewis and P. D. Tuttle, "The resistance and reactance of aluminum conductors, steel reinforced," *Amer. Inst. Elect. Eng. Trans.pt.III*,vol.77,pp 1189-1215, Feb.1959.
- [2] G. Gaba and M. Abbou-Dakka, "A Simplified and Accurate Calculation of Frequency Dependence Conductor Impedance," *Harmonics And Quality of Power, 1998. Proceedings. 8th International Conference on*, 14-16 Oct. 1998 939 - 945 vol.2
- [3] V. T. Morgan, "Effects of Alternating and Direct Current, Power Frequency, Temperature, and Tension on the Electrical Parameters of ACSR Conductors," *IEEE Transactions on Power Delivery, Vol.18, No.3*, pp 859-866, July 2003
- [4] A. R. Bergen, "Power System Analysis", Prentice Hall, 2000